LHCb Collaboration **LHCb 2001 –145 Rich**
Revised Dec. 2002

Measurement and monitoring of the refractive index of the Rich gaseous radiators in LHCb

M.Sannino, S.Cuneo, M.Ameri

Dipartimento di Fisica Universita` di Genova and INFN Sez. di Genova (Italy)

1) Introduction – Need of refractive index monitoring

As already pointed out [1,3] an important physical quantity that must be monitored in a Rich detector is the refractive index of the radiator. As well known, a charged particle which goes through a material with a velocity $v > c/n$ emits Cherenkov radiation with an emission polar angle with respect to the track given by

$$\theta_c = \arccos\frac{1}{n\beta} \qquad (1)$$

In a Rich detector the Cherenkov photons are focused on a photodetection plane where the positions of the photon hits on the so called Cherenkov Ring allow the angle θ_c to be reconstructed. As can be easily seen from (1) above the knowledge of the radiator refractive index is needed and therefore its measurement and monitoring. This is particularly true in case of a gaseous radiator where the refractive index monitoring, apart from the use in data analysis, is also a measure of stability of the radiator gas.

2) LHCb Rich requirements on the precision of the refractive index measurement

As specified in the LHCb RICH TDR[2] the radiator gases are C_4F_{10} for RICH 1 and CF_4 for RICH 2 and the resolutions and maximum values for the Cherenkov angles respectively are: in C_4F_{10} $\Delta\theta_c$ = 1.45 mrad, θ_c = 53 mrad with $n \approx 1.0014$ and in CF_4 $\Delta\theta_c$ = 0.58 mrad, θ_c = 32 mrad with $n \approx 1.0005$. From these data one can estimate that such resolutions require the knowledge of the refractive index n with a relative precision given by $\Delta n/n \approx 10^{-6}$ or, alternatively, the knowledge of the refractivity n-1 with a relative precision given by $\Delta(n-1)/(n-1) \approx 10^{-3}$

3) Experimental method – Fabry-Perot Interferometry

A classical experimental technique for the gas refractive index measurement is the Fabry-Perot interferometry performed with the method called Central Spot Pressure Scanning. Detailed descriptions of this classical method may be found in classical texts [4,5,6]. In what follows we recall the principles of the method. A Fabry-Perot interferometer is a device which relies on the interference of multiple beams. It consists (fig.1) of two partially transmitting mirrors precisely

aligned in order to form a reflective cavity. Incident light enters the Fabry-Perot cavity and undergoes multiple reflections between the mirrors so that the light can interfere with itself many times. If the frequency of the incident light is such that the constructive interference occurs within the Fabry-Perot cavity, the light will be transmitted. Otherwise destructive interference will not allow any light through the Fabry-Perot interferometer. The condition for constructive interference within a Fabry-Perot interferometer is that the optical distance between the two mirrors must equal an integral number of half wavelengths of the incident light. The constructive interference condition is therefore defined by the equation

$$nd\cos\theta = m\lambda \qquad (2)$$

where m is an integer expressing the order of interference, n is the refractive index of the medium between the two mirrors, d is the mirror separation and θ is the angle formed by the transmitted light with the normal to the mirrors.

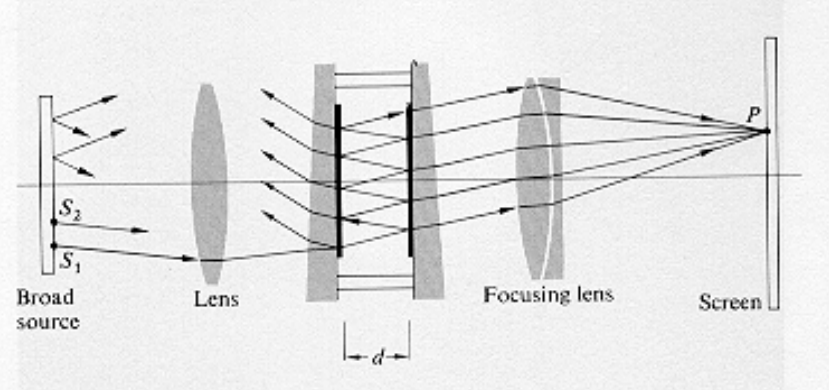

Fig.1

A Fabry-Perot interferometer generates a system of circular fringes at the infinity which are focused on a screen or a detector by means of a focusing lens. The transmitted intensity by a Fabry-Perot is

$$I_t = \frac{I_i[T/(1-R)]^2}{1+F\sin^2(\delta/2)} \qquad (3)$$

where I_i is the incident intensity, $F = 4R/(1-R)^2$ is the finesse, R,A and $T = 1-R-A$ are the reflectivity, absorption and transmittance of the mirrors and

$$\delta = \frac{4\pi d\cos\vartheta}{\lambda}n \qquad (4)$$

A typical interferogram is represented in fig.2,

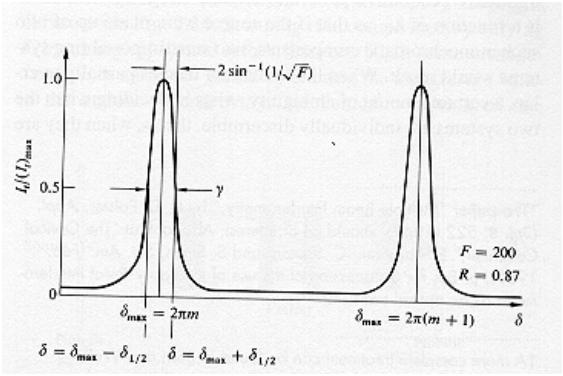

Fig.2

A widely used method to measure the refractive index of a gas is the so called *central-spot scanning* illustrated in Fig.3

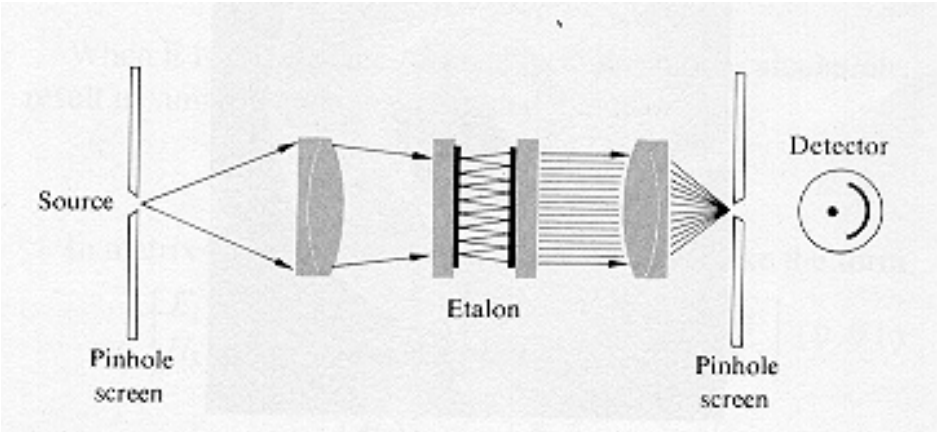

Fig.3

The whole Interferometer (called also Fabry-Perot Etalon) is closed in a gas tight vessel and a pinhole aperture is accurately positioned at the centre of the fringe pattern on the interferometer symmetry axis. The interferogram is scanned by means of a photoeletric detector, through the pinhole aperture, by varying the gas pressure and hence the refractive index between the mirror plates. In a typical measurement the Fabry-Perot vessel is evacuated at the beginning ($p \approx 0$) and at the end is filled with the gas at the pressure at which its refractive index must be measured. Obviously the temperature must be kept

constant during this process. As the pressure of the gas is increased up to its final value P, the number of interference fringes N(P), from vacuum to final pressure, is counted and, as can be easily deduced from (4) with $\theta = 0$, a measurement of the refractivity at the final pressure, $n(P)$-1, is obtained:

$$(n(P)-1) = \frac{\lambda}{2d}\mathrm{N}(P) \tag{5}$$

where λ is the wavelength of the radiation used.

3.1) Sensitivity and Precision in Fabry-Perot Spectroscopy

Defining the **Reflectivity Finesse** as

$$N_R = \frac{\pi\sqrt{F}}{2} \tag{6}$$

it can be demonstrated [4,5,6] that in a Fabry-Perot Interferometer this quantity is related to γ, the FWHM of the interference peak, by the relation

$$N_R = \frac{2\pi}{\gamma} \tag{7}$$

So typical quantities defining the sensitivity of a Fabry-Perot Interferometer are the **minimum resolvable bandwidth**,

$$(\Delta\nu)_{\min} = \frac{c}{N_R 2dn} \tag{8}$$

i.e. the minimum frequency difference needed to resolve two different frequencies, and the **Free Spectral Range (FSR)**, i.e. the separation in terms of frequency between adjacent orders of interference.
It can be demonstrated that

$$(\Delta\nu)_{FSR} \cong \frac{c}{2dn} \tag{9}$$

and so, from (8) and (9), for a fixed frequency ν_0

$$\frac{(\Delta\nu_0)_{FSR}}{(\Delta\nu_0)_{\min}} = N_R \tag{10}$$

However, besides the reflectivity, the resolving power of a Fabry-Perot Interferometer is also affected by the flatness of the mirrors and this effect is described[9,10] by means of the **Defect Finesse** N_D which is defined by $m/2$ when the departures from the flatness are measured as a fraction of the reference wavelength λ/m. It is important to remark that a flatness of $\lambda/100$, giving $m = 100$ for the 633 nm red line of the He-Ne laser, gives only $m = 24$ for e.g. a 152 nm UV line so that the defect finesse is only 12 in case of UV instead of 50 for red.
Taking into account both the effects of the reflectivity and the departure from flatness of mirrors a **Recorded Finesse** (or **Effective Finesse)** N is defined and it can be shown that eq. (10) becomes

$$\frac{(\Delta\nu_0)_{FSR}}{(\Delta\nu_0)_{\min}} = N \tag{11}$$

where

$$N = (N_D^{-2} + N_R^{-2})^{-1/2} \tag{12}$$

3.2) Sensitivity in a Fabry-Perot Central Spot Pressure Scanning refractivity measurement

If errors on temperature T, final pressure P and distance between etalon plates are negligible as considered by Abjean et al.[7] (a thorough discussion on this point will follow later) the relative error on refractivity is

$$\frac{\Delta(n-1)}{n-1} = \frac{\Delta(\mathrm{N}(P))}{\mathrm{N}(P)} \tag{13}$$

In what follows we assume an etalon air gap d = 1 cm and, again, following Abjean et al.[7], λ_0 = 206.82 nm, $(n - 1) = 523.6 \times 10^{-6}$, an indetermination on fringes counting $\Delta(\mathrm{N(P)}) = 1/20$ fringe on an individual record of fringes[1]. With these data inserted in eq. (5) the number of counted fringes is

$$\mathrm{N}(P) = 50.63 \tag{14}$$

and from eq. (13)

$$\Delta(n\text{-}1)/(n\text{-}1) \cong (1/20)/50.63 \approx 10^{-3} \tag{15}$$

[1] It's worth to note that in Abjean et al. work the interferometer finesse value is N=6.3 at about 150 nm (N_R = 7.5 at 150 nm and N_D = 12 at 152 nm)

obtaining the required precision (see above, par.2) for the measurement. It is worth to remark that this is a pessimistic estimate as a statistical treatment of a number of scans (e.g. ~ 12 scans) will for sure reduce the relative error on refractivity (See Abjean et al.[7]) .
In a central spot pressure scanning with monochromatic light the effect of a higher finesse value of the etalon is relevant to improve the sharpness of the interferogram peaks structure and, as a consequence, a lower error in the fringe counting. This is evident in two different papers[8,9] by Bideau-Mehu et al. (same authors as in [7]) where interferograms with an improved finesse[9] and with a worse finesse[8] are reported.

3.3) Effect of Temperature and Pressure on the precision of refractive index measurement

Normally the operational stability of a Rich is much affected by the temperature and pressure stabilities of the gas radiator. As well known[4] the dependance on temperature T and pressure p of the refractive index of a dilute gas is deduced by the Clausius-Mossotti (also known as Lorentz-Lorenz) equation in the approximation of a perfect gas and consequently well described by the equation

$$n^2 \cong 1 + 3\frac{A}{R}\frac{p}{T} \qquad (16)$$

where A and R are respectively the molar refractivity and the gas constant. The relative variation of the refractive index n is found differentiating eq. (16) above and assuming the values $p \approx 1100$ mbar, $T \approx 300$ K, monitored with precisions $\Delta p = 0.1$ mbar, $\Delta T = 0.1$ K, as foreseen in LHCb Technical Proposal[1]. With the above data, in a wavelength interval between 200 and 400 nm, a relative variation $\Delta n/n \approx 0.2 \times 10^{-6}$ is obtained with the corresponding value in refractivity $\Delta(n-1)/(n-1) \approx 0.2 \times 10^{-3}$. This result is perfectly compatible with the requirements on the precision of the refractive index measurement quoted in par. 2 above. Moreover, confirming what has been assumed in par. 3.2 above, provided that the interferometer vessel is monitored and kept stable to a precision Δp and ΔT, the contribution of pressure and temperature variation to the precision of the refractivity measurement, obtained from eq. (15) above, is actually negligible. These considerations allow in turn the value of refractivity, measured by means of the interferometer, to be scaled to the radiator in the RICH vessel within the required precisions.

4) Proposed refractive index monitoring system in LHCb RICH

In LHCb we propose a refractive index monitoring for the RICH gas radiators by means of the Fabry-Perot central spot pressure scanning technique above described. The wavelength range should lie in the interval $200nm \le \lambda \le 400nm$, due to the quartz window cut off at low wavelengths. Our present aim is to build a prototype refractometer in order to verify the feasibility of the method, eventually in view of its insertion in the on line monitoring system.
The main aim of the radiator gas monitoring is to verify the refractivity vs. wavelength dependance, usually parametrized by the well known Sellmeier formula (see e.g.[7])

$$n - 1 = \frac{A \times 10^{-6}}{\lambda_0^{-2} - \lambda^{-2}}$$

where λ_0 and A are characteristic parameters of the gas.
To accomplish this a monochromator in front of the entrance window of the Fabry-Perot vessel will be used as a source of monochromatic light.

In summary the refractometer will be composed as follows.

4.1) light source: a good light source for these applications is a Platinum hollow cathode lamp. A hollow cathode lamp accomplishes the requirement of generating narrow emission lines, so each line shows a good spectral purity and enough coherence length for interferometer application. These lamps (fig. 4) are commercially available from many manufacturers (e.g. Hamamatsu, Varian, Cathodeon etc.). A typical Pt Hollow cathode lamp spectrum is reported in a paper by G.H Mount et al.[11].

fig. 4

4.2) Monochromator: The monochromator will be a model HR 250 by Jobin Yvon and its characteristics are summarized in fig.5 below reproducing the relevant page of its user manual.

fig.5 Monochromator Characteristics

Characteristics

- Asymmetric Czerny-Turner type optical configuration,
- Focal length: 245.761 mm,
- Spectral range: 190 nm - 40 µ,
- Dispersion: 3 nm/mm at 500 nm with 1200 gr/mm grating,
- Spectrograph version: 25 mm spectral field,
- Aperture: F/4.1,
- Resolution: better than 0.1 nm at 500 nm with 1200 gr/mm grating.
- Slits: - Straight,
  - Fixed (width 0.5 - 1 - 2 mm) or continuously adjustable from 0 to 2 mm,
  - Height adjustable from 2 to 8 mm.
- Included angle: 20.00 degrees,
- Display: 4-digit mechanical counter,
- Manual or stepper motor scanning,
- Dimensions: 370 x 355 x 216 mm,
- Weight: 10 kg,
- Optional nitrogen purge.

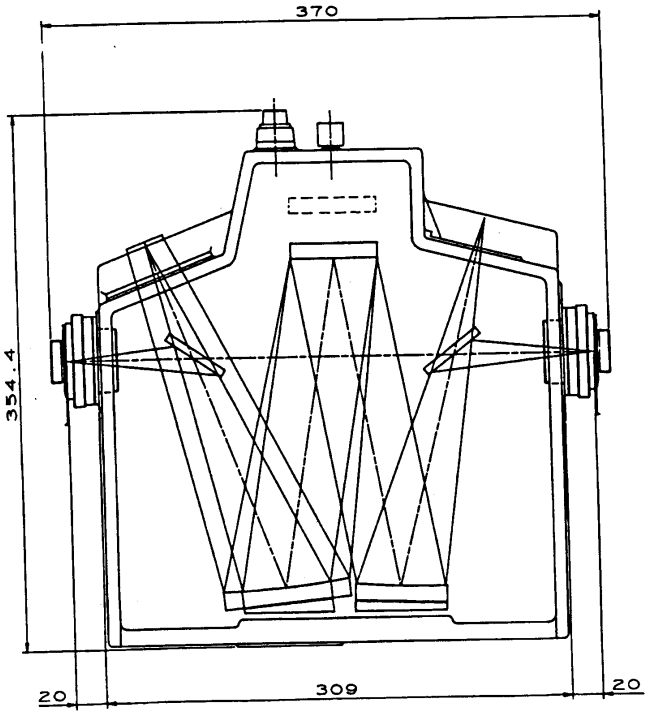

4.3) Refractometer

In what follows we present the design of a prototype refractometer, based on the considerations of the above paragraphs. This, in a first phase, will be used to implement the measurement procedure and to perform the first measurements. From the experience gained with it a definitive system, somehow a replica / upgrade of this prototype refractometer, to be eventually installed in the on-line monitoring system of the experiment, will be realized.

a) general assembly

In fig.6 the general assembly of the refractometer inside the gas tight vessel is represented. The light from the monochromator enters from the left on the drawing through a diaphragm (possibly a tunable iris) and, by means of a condensing lens system, a parallel beam illuminates the etalon plates. The output light is then focused again through a diaphgram (a tunable iris) on a photomultiplier photocathode. The photomultiplier is a Hamamatsu R943-02 especially foreseen for photon counting with a wide spectral range (160 to 930 nm)[(12)]. As above mentioned and clearly represented in the drawing, the Fabry-Perot etalon is enclosed in a gas tight vessel in order to allow the pressure scanning starting from vacuum up to the normal pressure. The light enters and leaves the sampling cell through MgF_2 windows, transparent to UV, mounted on appropriate flanges. These windows are produced by vacuum component producers, as Caburn, and are reported in commercial catalogues. All condensing and focusing lenses are of course UV transparent and are selected from Crystran and Newport productions. Special calibrated valves for constant laminar flow at gas inlet and a thermostatic control in order to keep a stable temperature are foreseen. Again temperature and pressure gauges with the needed precisions (0.1 K and 0.1 mbar) are standard components commercially available.

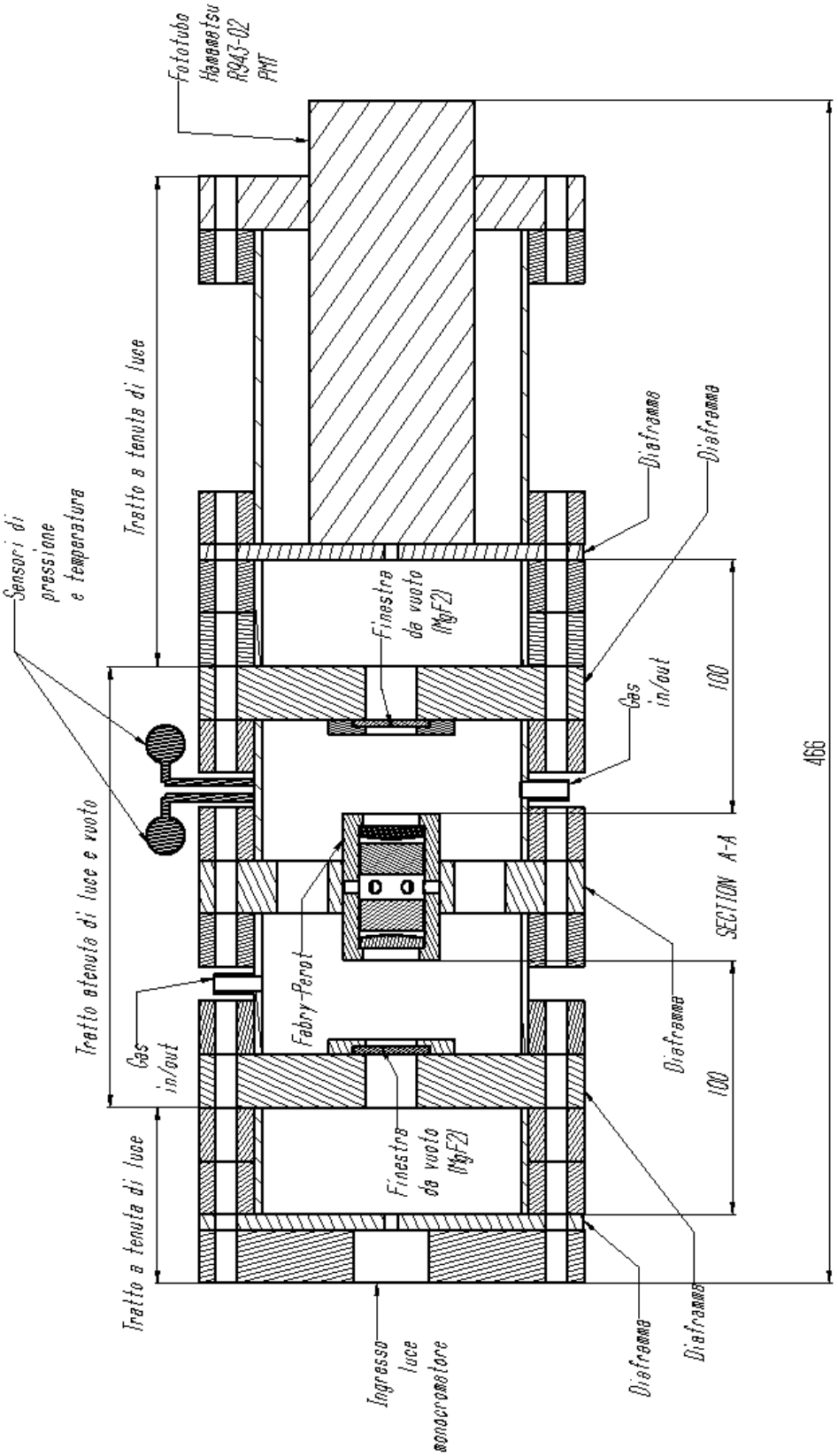

Fig.6 General Assembly of the refractometer body

b) Fabry-Perot Etalon

A problem which arises with Fabry-Perot Etalon plates is the fact that at wavelengths lower than 240 nm there is limited choice of dielectric coating materials that can be used for the Fabry-Perot Etalon plates. Infact, in the visible and in the near UV there are materials with negligible losses, as oxides (e.g. titanium dioxide, TiO_2), with 99% reflectivities and 20 nm reflectivity bandwidth, therefore suitable for high reflectivity-finesse etalons. Moreover at such wavelengths defect finesse is not too critical and, as a result, a good **Effective Finesse**, is attainable. At wavelengths lower than 240 nm, towards deep UV, this is no longer the case. The choice of suitable materials is severely limited, as so many otherwise suitable candidates absorb strongly. For the few materials that can be used the refractive indices are never ideal. For example, at 190 nm fluorides (e.g. MgF_2) must be used as coatings (see also Bideau-Mehu et al[8,9]), as all of the more useful oxides absorb strongly. Refractive index shortcomings mean that the maximum reflectivity attainable is about 95% over a bandwidth of about 5 nm. Also the **Defect Finesse** incidence becomes an important factor at such short wavelengths. Therefore, in order to be able to perform a measurement over the whole range of λ, i.e., from 200 nm up to 400 nm, two different, but mechanically interchangeable, Fabry-Perot etalons are needed. One of them will be used in the range $200 \le \lambda \le 240nm$ and the other in the range $240 \le \lambda \le 400nm$. In fig.7 the mechanical configuration valid for both etalons is shown while in Figs. 8 and 9 the Etalon Specifications, respectively for the two wavelength ranges, are reported.

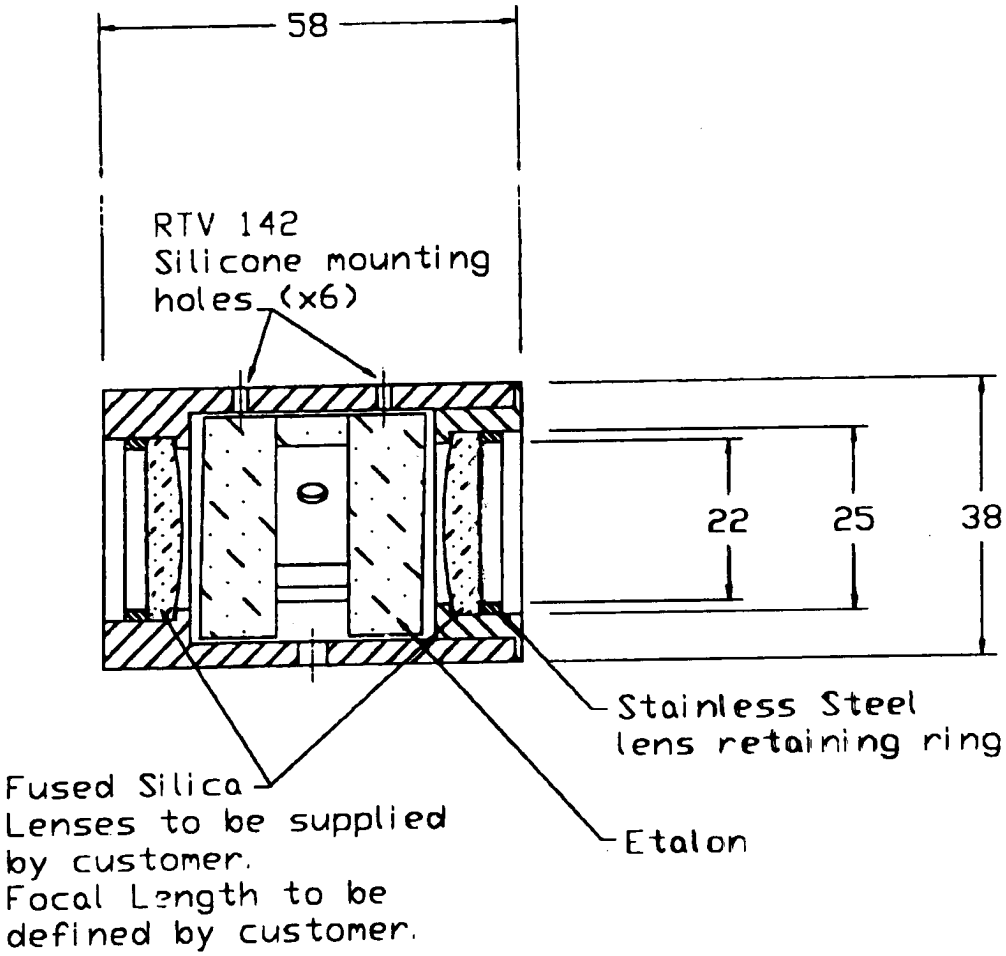

Fig.7 Geometrical configuration of the Etalon

SLS Optics Ltd

Etalon Specifications

18/05/01

Mario Sannino
University of Genoa
Department of Physics
Italy

Reference: RFQ 14/05/01
Description: 20mm CA air-spaced etalon. 10mm air gap. Effective finesse ~40, over 5mm aperture

Wavelength: 202.50nm
Clear Aperture: 20.00mm
Effective Aperture: 5.00mm
FSR: 0.0020nm - 0.4999cm-1 - 14.985GHz
Spacing: 10.000mm - Refractive Index: 1.0003
Flatness: Lamdba/150 @ 633nm
Parallelism: Lambda/100 @ 633nm
Surface Roughness: 0.40nm
Beam Divergence: 0.10milliradians

Coating Reflectivity: 95.0%
Reflection Coating Loss: 1.00%
Antireflection Coating Loss: 2.00%

Reflectivity Finesse: 61
Effective Finesse: 43 over 5.00mm aperture

Peak Transmission: 44%

Fig.8 Optical Characteristics of a possible Etalon in the range $200 \leq \lambda \leq 240nm$

SLS Optics Ltd
Etalon Specifications

18/05/01

Mario Sannino
University of Genoa
Department of Physics
Italy

Reference: RFQ 14/05/01
Description: 20mm CA air-spaced etalon. 10mm air gap. Effective finesse ~70, over 6mm aperture

Wavelength: 390.00nm
Clear Aperture: 20.00mm
Effective Aperture: 6.00mm
FSR: 0.0076nm - 0.4999cm-1 - 14.985GHz
Spacing: 10.000mm - Refractive Index: 1.0003
Flatness: Lamdba/150 @ 633nm
Parallelism: Lambda/100 @ 633nm
Surface Roughness: 0.40nm
Beam Divergence: 0.10milliradians

Coating Reflectivity: 97.0%
Reflection Coating Loss: 0.10%
Antireflection Coating Loss: 0.60%

Reflectivity Finesse: 103
Effective Finesse: 72 over 6.00mm aperture

Peak Transmission: 65%

Fig.9 Optical Characteristics of a possible Etalon in the range $240 \leq \lambda \leq 400nm$

Conclusions

As well known in a Rich detector a good precision measurement and monitoring of the gas radiator refractive index is needed in order to reconstruct the Cherenkov angle for the different particles
A system based on Fabry-Perot interferometry, in order to monitor and measure the refractive index of CF_4 of the LHCb Rich2 with the needed precision $\Delta n / n \approx 10^{-6}$, has been devised and, after a detailed study of the attainable measurements accuracies, a possible implementation of it has been presented.

Acknowledgments

One of us (MS) is deeply grateful to C. D'Ambrosio, V. Gracco, P. Mazzinghi, A. Petrolini and O.Ullaland for many interesting, stimulating discussions and suggestions.

References

1) "LHCb Technical Proposal", CERN/LHCC 98-4, LHCC/P4, 20 Feb., 1998
2) "LHCb RICH TDR", CERN/LHCC/2000-0037,LHCb TDR 3 7Sep., 2000
3) C. D'Ambrosio et al., "Monitoring, Alingnment and Control of the RICH Detectors", LHCb Internal Note 2000-80 RICH, 6 Sept., 2000
4) Born and Wolf, "Principles of Optics", 7th ed.
5) W. Ewart Williams, "Applications of Interferometry"
6) J.M. Vaughan, "The Fabry-Perot Interferometer"
7) R. Abjean, A. Bideau-Mehu, Y. Guern, "Refractive Index of Carbon Tetrafluoride (CF_4) in the 300-140 nm range", Nucl. Instr. and Meth. **A292**(1990)593
8) A. Bideau-Mehu, Y. Guern, R. Abjean, A. Johannin-Gilles, "MgF_2 Fabry-Perot Etalon Plates for the Vacuum Ultraviolet", Appl. Opt. **15**(1976)2626
9) A. Bideau-Mehu, Y. Guern, R. Abjean, A. Johannin-Gilles, "Improved MgF_2 Etalon Plates for Fabry-Perot Interferometry in the VUV from 170 to 138 nm", J.Phys. E: Sci. Instrum. **13**(1980)1159
10) P.S. Nylen,"On the Scanning Fabry-Perot Interferometer", Physica Scripta **8**(1973)81
11) G.H. Mount, G. Yamasaki, V. Fowler, W.G.Fastie, "Compact Far Ultraviolet Emission Sourca with Rich Spectral Emission 1150-3100 Angstrom", Applied Optics **16**(1977)591
12) Hamamatsu Photomultiplier Tubes Catalog